Vol. 68, pp. 105-115, 1986

Naturally Occurring Nonneoplastic Histopathological Lesions in the Female SENCAR Mouse

by Robert M. Kovatch,* Gary L. Knutsen,* and Merrel Robinson†

Lesions that were considered naturally occurring were surveyed in female SENCAR mice used in short-term bioassays. These lesions were encountered in selected target organs and in organs and tissues with gross lesions encountered at necropsy. The genitourinary system was the most frequent site for lesions; cystic ovaries, cystic endometrial hyperplasia, and glomerulonephritis were commonly encountered in this system.

Introduction

SENCAR mice have been developed for susceptibility to skin tumor response using a two-stage tumor induction regimen (*1,2*). A paucity of information is available on the naturally occurring lesions in this strain. It is the purpose of this paper to present a survey of lesions encountered in control and treated female SENCAR mice used in short-term EPA Carcinogenesis Testing Matrix Studies. Inasmuch as only target tissues and organs with gross lesions were examined microscopically, incidence data for the various lesions could not be determined.

Materials and Methods

Female SENCAR mice were obtained at 5 to 7 weeks of age from Harlan-Sprague Dawley Laboratories, Inc. (Indianapolis, IN). During the experiment, mice were grouped 10 per cage and fed Purina Laboratory Chow and water *ad libitum*.

Mice on these studies included control and test animals that were approximately 8 weeks old at experiment initiation and were placed on a 30- or 52-week treatment phase. Tissues examined included selected target organs and all organs or tissues with gross lesions encountered in a complete necropsy of each animal. Organs and tissues were fixed in 10% formalin, processed through paraffin, sectioned at 5 or 6 μm and stained with hematoxylin and eosin for microscopic examination.

*Pathology Associates, Inc., 10075 Tyler Place, Hyatt Park II, Ijamsville, MD 21754.

†Toxicology and Microbiology Division, U.S. Environmental Protection Agency, 26 W. St. Clair St., Cincinnati, OH 45268.

Results and Discussion

Digestive System

Liver. Amyloidlike deposits were found in the liver of both test and control mice (Fig. 1) and appeared as slightly eosinophilic amorphous deposits located around sinusoids. Deposits were most intense in peripheral portions of the lobule. Such lesions were usually associated with inflammatory processes elsewhere in the body, such as clitoral gland abscesses and, in skin paint studies, an extensive inflammatory reaction associated with the skin lesion. Generally, the amyloidosis was systemic and involved multiple organs as described below. Amyloidosis is not an uncommon lesion in mice and has been reported in a variety of mouse strains (*3*).

In this age group, foci of cellular alteration in the liver considered to have preneoplastic significance were uncommon. However, these foci need to be differentiated from foci of vacuolated, usually lipoid-laden cells that involve one or a few hepatic lobules found near the cleft of the median lobe (Fig. 2). In our experience, the latter lesion is not age-related, is encountered in several species, and does not have any preneoplastic significance.

Inflammatory cell infiltration or hematopoietic cell proliferation commonly occurred in the liver. The inflammatory reactions appeared as aggregates of lymphocytes and macrophages distributed randomly throughout the liver. These reactions have not been associated with a specific etiological agent in our studies. Chronic reactions commonly have brown pigment, probably hemosiderin or bile, present in small lobes; the presence of bile was attributed to bile duct obstruction. Hematopoietic cell proliferation presented as variably

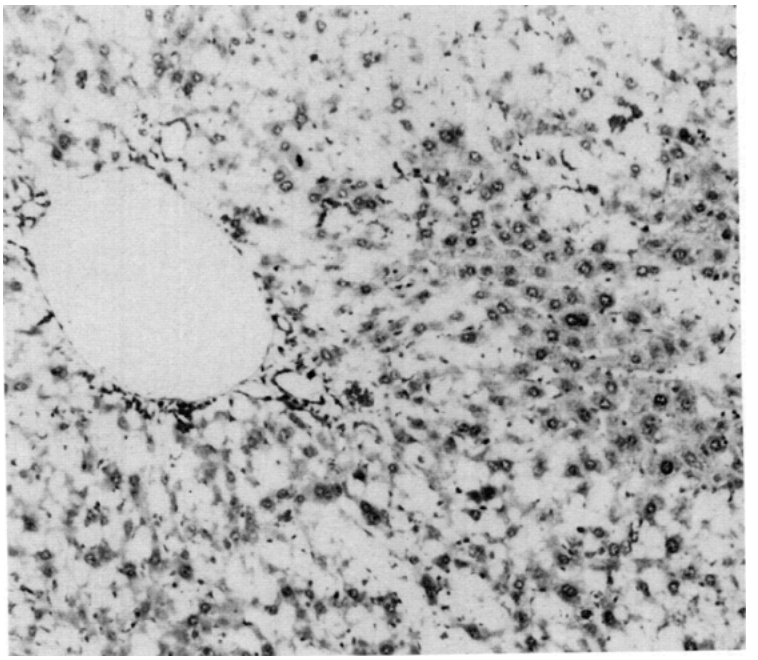

FIGURE 1. Amyloidlike deposits primarily involving peripheral portions of the liver lobule (H & E, ×260).

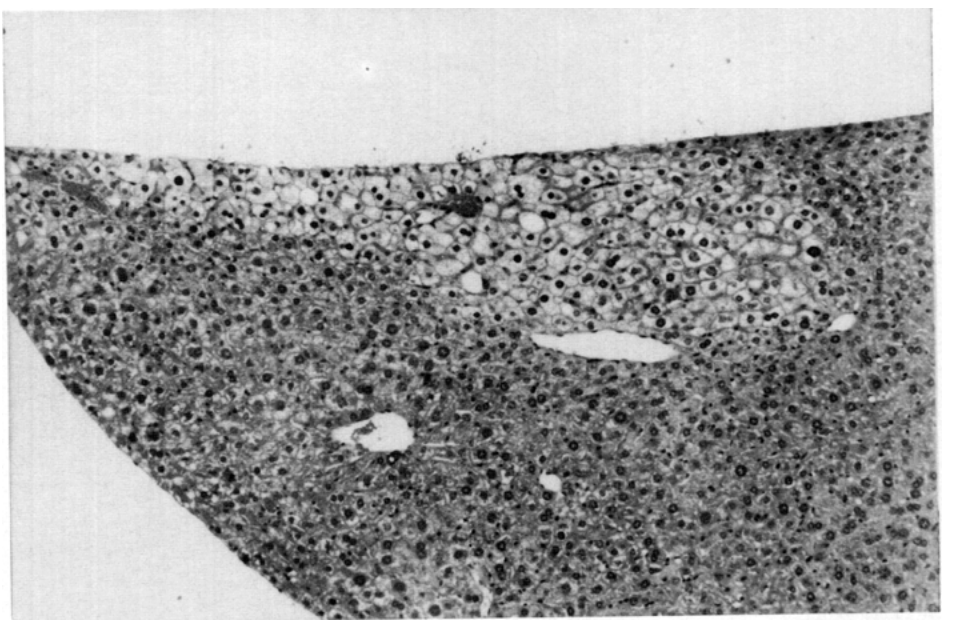

FIGURE 2. Focus of vacuolated hepatocytes located near the capsule of the median liver lobe (H & E, ×130).

sized erythrocytic, granulocytic, or mixed foci in sinusoids of the liver. These foci were common in tumor-bearing mice or in mice with inflammatory processes elsewhere in the body. The hematopoiesis was extensive in many instances, giving the appearance of leukemia as described by Long (*4*).

Strangulation of the liver lobes, or portions thereof, was seen both grossly and microscopically. Some of these lesions resembled pancreatic masses. Microscopically, such areas of ischemic liver necrosis were frequently surrounded by a prominent connective tissue capsule (Fig. 3).

Other lesions encountered included biliary cysts, fatty change in debilitated animals, focal sinusoidal ectasia, and lymphocytic or plasmacytic infiltrates of portal areas.

Pancreas. Focal acinar cell atrophy was observed. The lesion was characterized by depletion or absence of

FIGURE 3. Ischemic liver necrosis centrally, surrounded by a connective tissue proliferation at the capsular surface, secondary to strangulation (H & E, ×120).

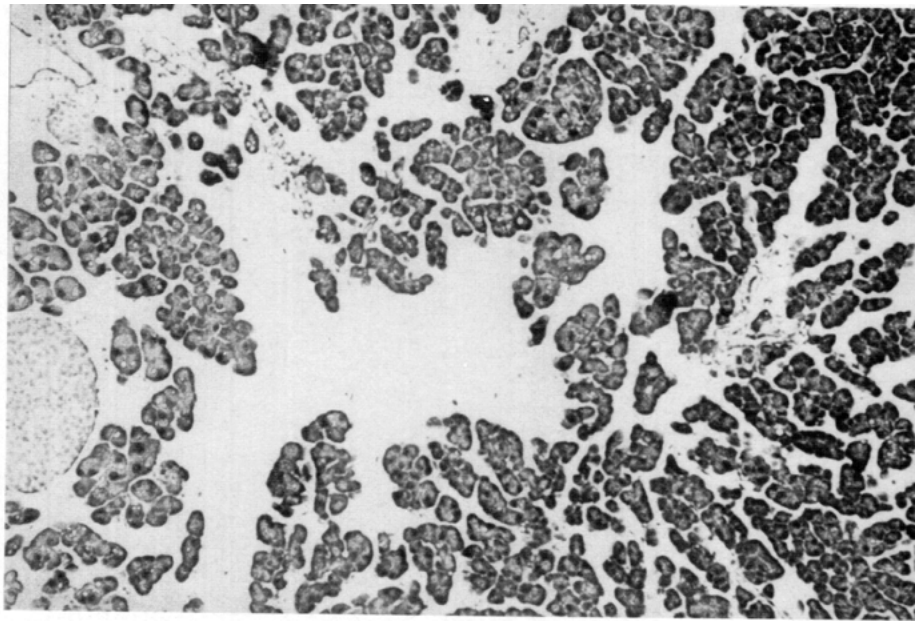

FIGURE 4. Acini depleted of zymogen granules in a pancreas described grossly as being white (H & E, ×120).

acinar cells with only pancreatic islets and ductules remaining in some cases. Amyloidlike deposits were occasionally observed histologically, appearing diffusely in interstitial areas but tending to concentrate near small vessels. Also seen grossly were pancreata with a diffuse white appearance. Zymogen granule depletion was the prominent microscopic feature (Fig. 4). Focal islet hyperplasia was the only other alteration found in this survey.

Digestive Tract. Inflammatory reactions were infrequent. Small mucosal erosions and ulcerations were occasionally found (Fig. 5). Hyperplasia of gut-associated lymphoid tissue of the small and large intestine was infrequently seen. Pinworms in the lumen of the large intestine were also infrequently identified.

An unusual glandular hyperplasia of the duodenal mucosa was observed. Only a few examples were found, and they occurred in test animals. The lesion was characterized by a segmental hyperplasia of the glandular elements with ectasia of glands near the base (Fig. 6).

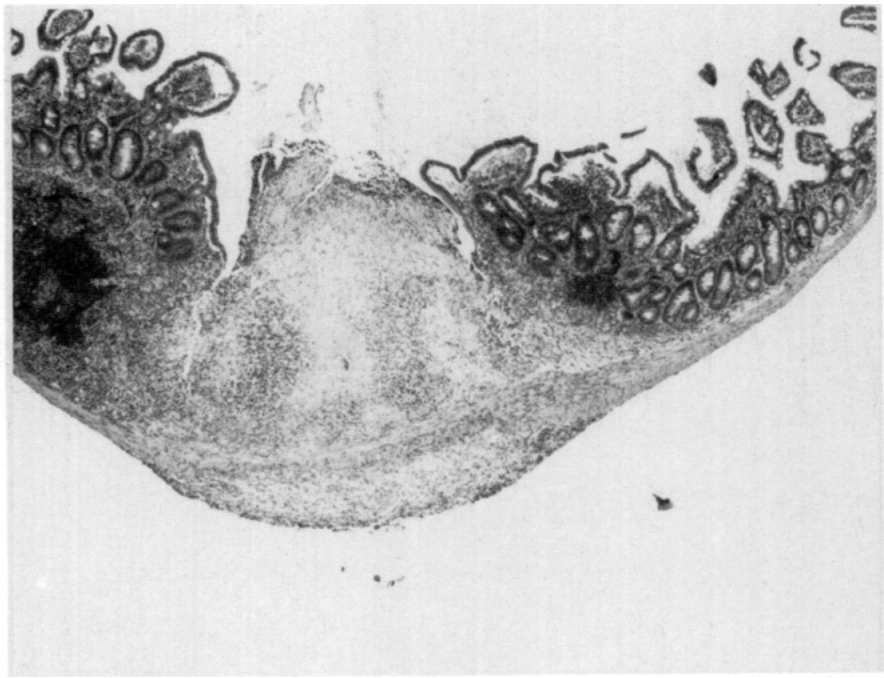

FIGURE 5. Ulcerated mucosa of the ileum. The serosa is thickened by inflammatory cell infiltration and connective tissue proliferation (H & E, ×52).

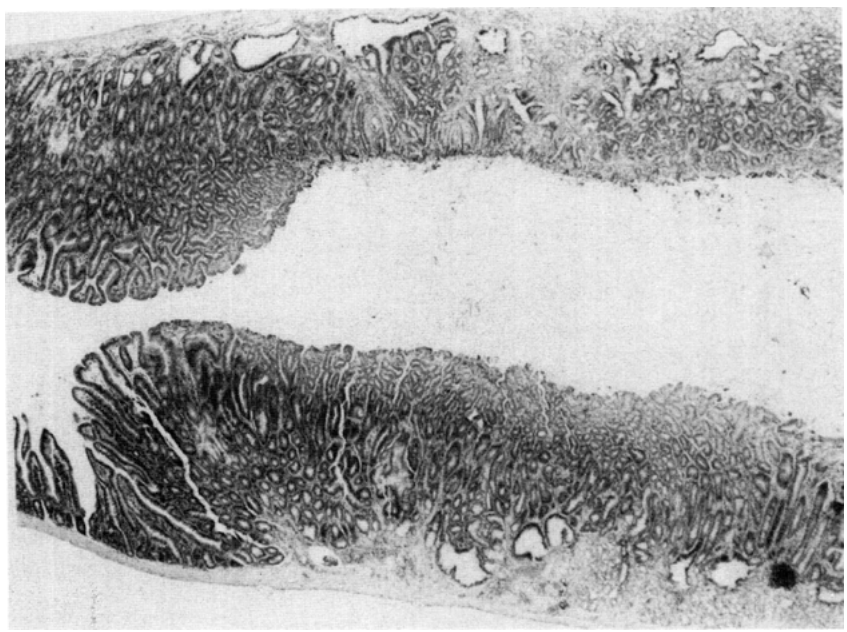

FIGURE 6. Segmental mucosal hyperplasia of the duodenal mucosa. Glands are ectatic near the base (H & E, ×26).

Endocrine System

Adrenal Gland. Adrenal gland focal segmental hyperplasia extending from the zona granulosa and hypertrophy of small nests of cortical cells were occasionally observed. More frequently, segmental or diffuse hyperplasia of spindle cells extending from the adrenal capsule was seen (Fig. 7). Such subcapsular hyperplasia is common in mice of several strains (*5*).

Thyroid. Gross lesions were not observed. Occasionally, the thyroid was captured in sections of the upper respiratory tract. Small epithelial-lined cysts, considered embryonal remnants of the ultimobranchial duct, were found. The only other abnormality observed

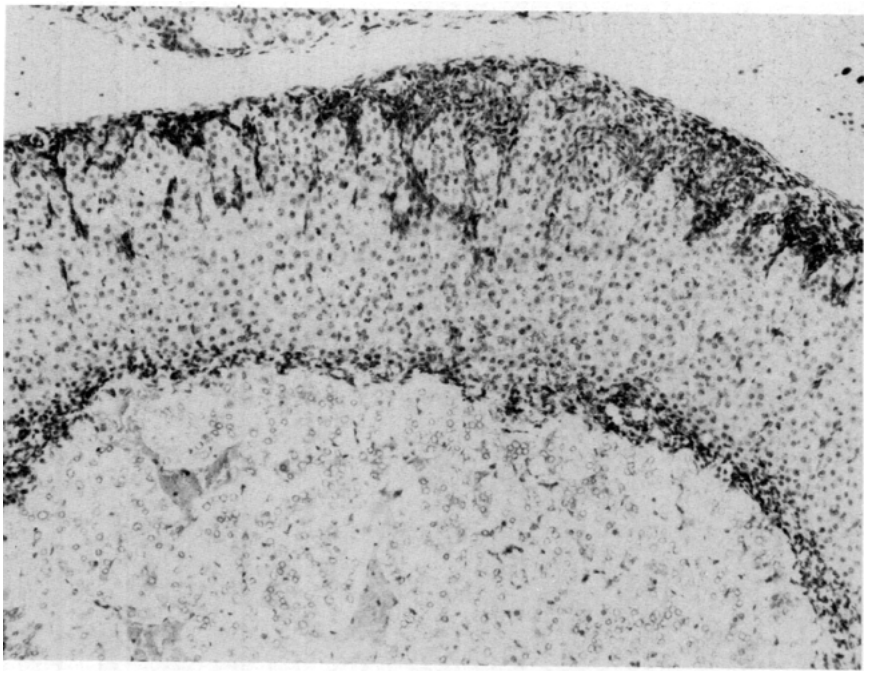

FIGURE 7. Subcapsular cell hyperplasia of the adrenal with nests of hyperchromatic cells extending to the zona fasciculata (H & E, ×120).

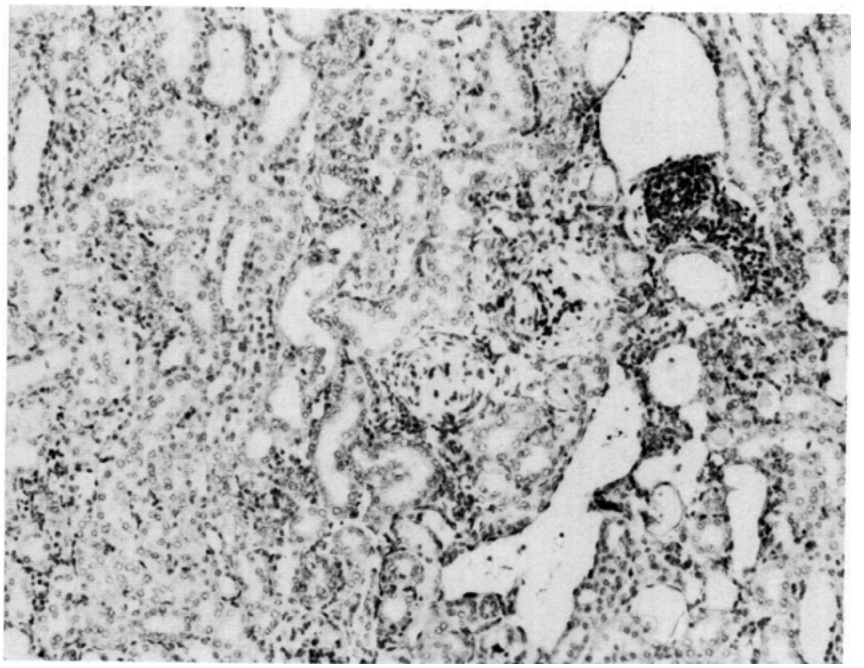

FIGURE 8. Sclerotic glomeruli, tubular casts, and perivascular inflammatory infiltration in kidney (H & E, ×260).

was the distention of individual follicles, which was diagnosed as follicular cysts.

Genitourinary System

Kidney. The most frequent finding was segmental or diffuse, usually minimal or mild, glomerulonephritis. It was observed in both control and treated animals. In severe cases, the lesion was characterized by mesangial hypercellularity, sclerosis of glomeruli with adhesions to Bowman's membrane, fibrosis of Bowman's capsule, tubular casts, and interstitial inflammatory infiltrates (Fig. 8).

Agenesis and renal hypoplasia, considered congenital

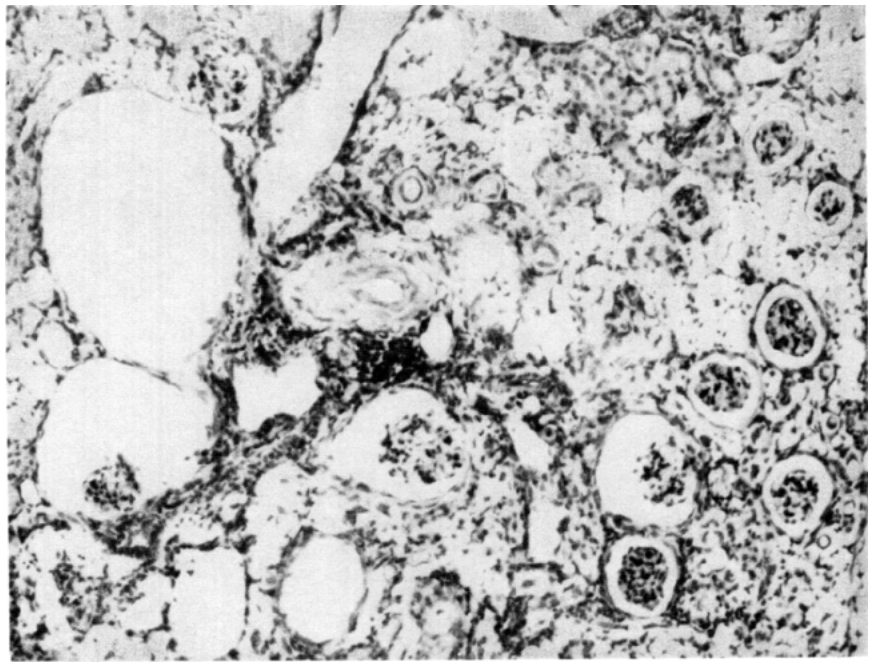

FIGURE 9. Kidney with marked cortical atrophy. A small nest of more normal-appearing renal tubules is located near the top (H & E, ×260).

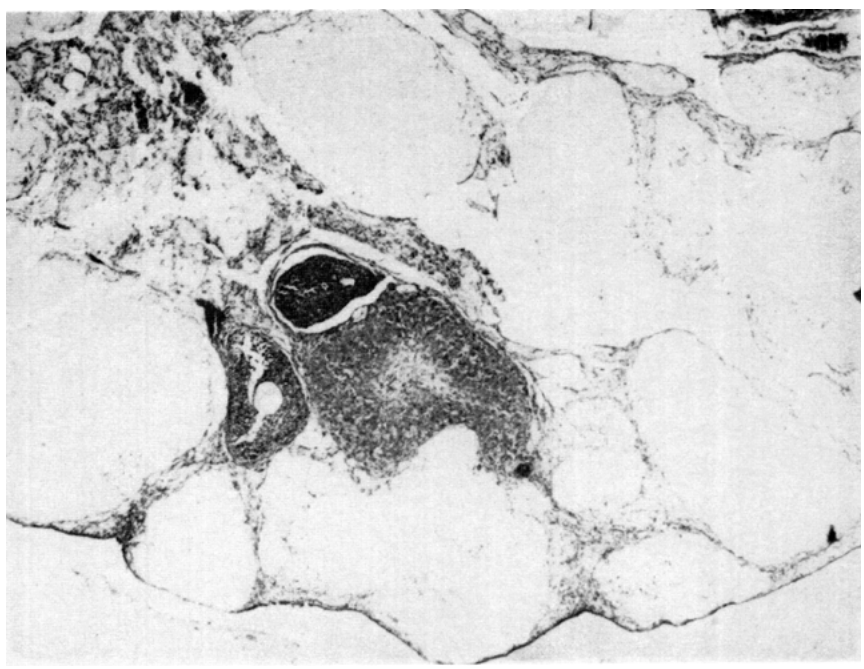

FIGURE 10. Amyloidlike deposits in the ovary. The principal deposits are in the corpora lutea (H & E, ×52).

malformations, were not unusual findings. Hypoplastic kidneys were characterized by marked cortical depletion, with only atrophic glomeruli and occasional nests of normal-appearing cortical tubules remaining (Fig. 9). Plasmacytic and lymphocytic infiltrates in the medulla were intense in some cases.

Other renal lesions included cortical cysts, hydronephrosis, perivascular inflammatory infiltrates, nephrocalcinosis, pyelonephritis, and hyperplasia of the pelvic epithelium.

Ovary. Amyloidlike deposits, an infrequent finding, were observed in areas of the ovary corresponding to

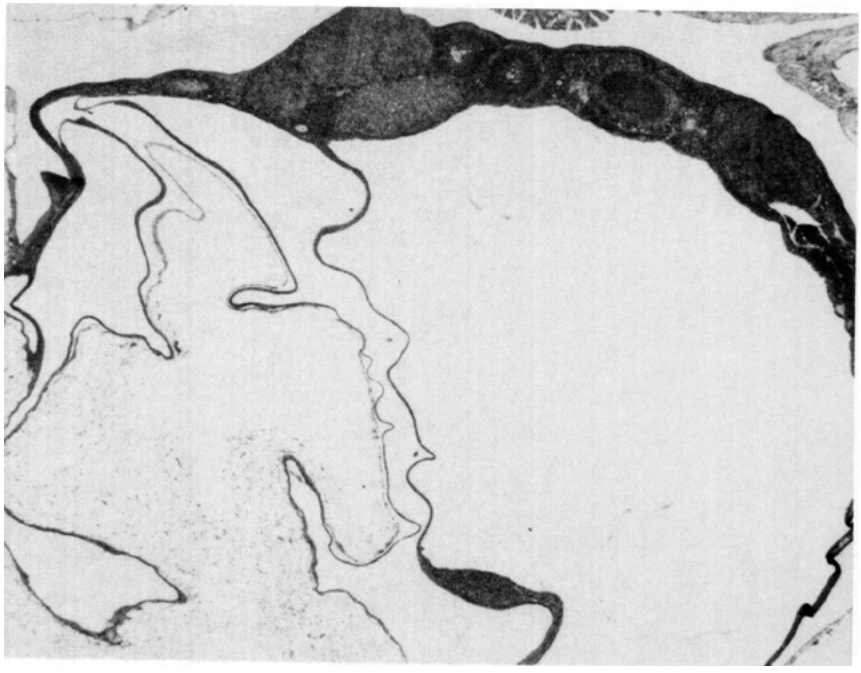

FIGURE 11. Ovarian tissue essentially replaced by a multiloculated cyst (H & E, ×52).

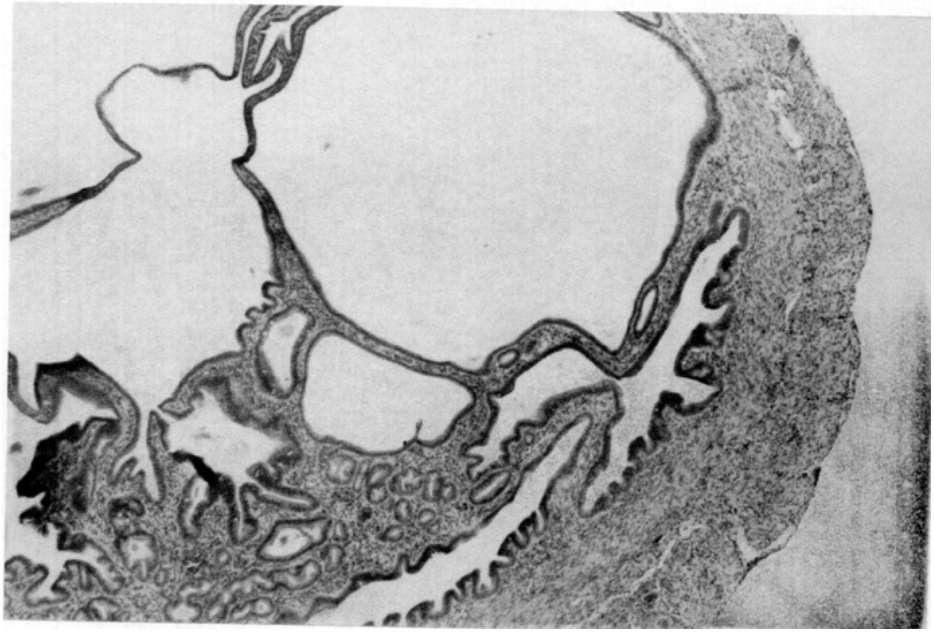

FIGURE 12. *Cystic endometrial hyperplasia of the uterus* (H & E, ×26).

corpora lutea (Fig. 10). This finding may represent a genetic susceptibility in SENCAR mice, since it is common in CD-1 mice (*6*).

The appearance of ovarian cysts or hematocysts is exceedingly common. The majority of these cysts resulted from distension of the ovarian bursa with clear, tan, or red fluid. Less frequently, Graffian follicles or corpora lutea were cystic. The origin of the cyst was usually not identifiable. Microscopically, a portion or the entire ovary was sometimes

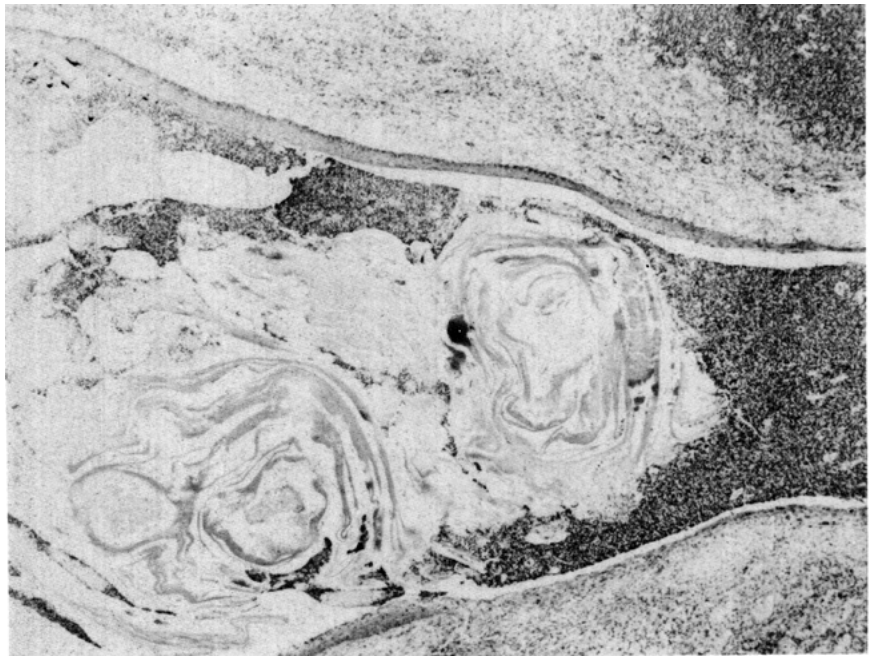

FIGURE 13. Inflammation and abscessation of the clitoral gland. The gland is distended with keratinaceous debris and purulent exudate (H & E, ×52).

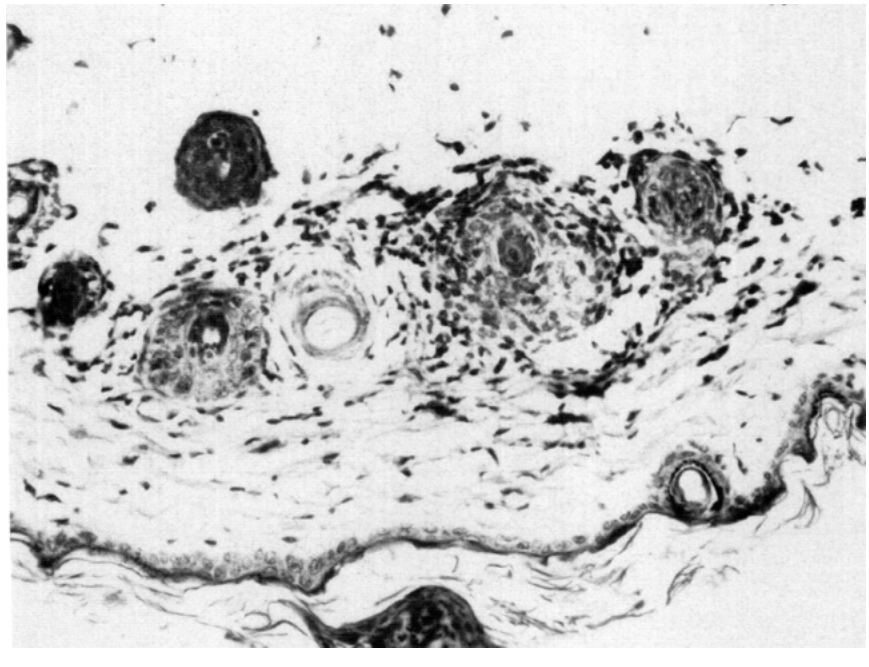

FIGURE 14. Perifollicular inflammatory infiltration involving the dermis. A small quantity of exudate is located on the epidermis (H & E, ×260).

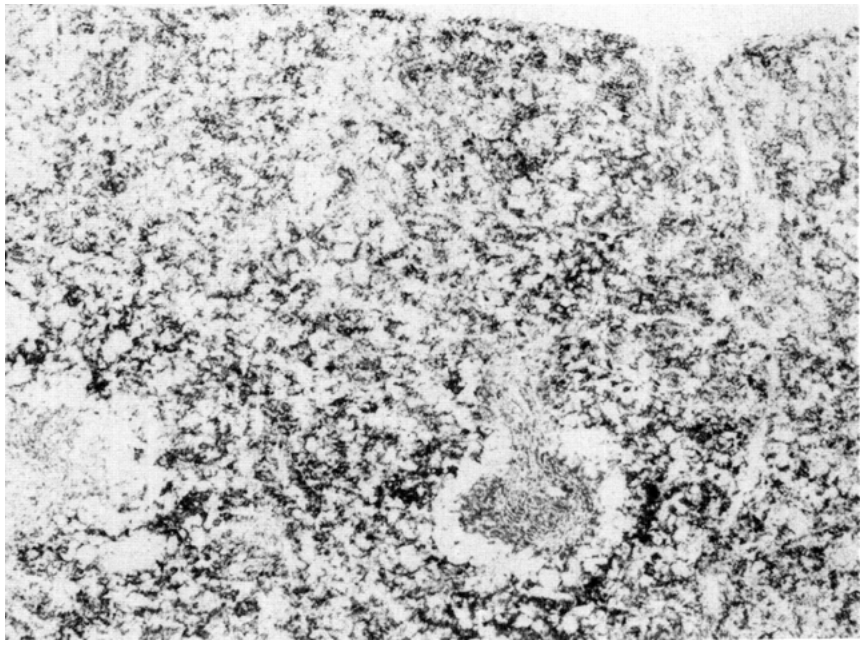

FIGURE 15. A spleen with perifollicular deposits of amorphous amyloidlike material. The red pulp is hypercellular due to hematopoietic cell proliferation (H & E, ×260).

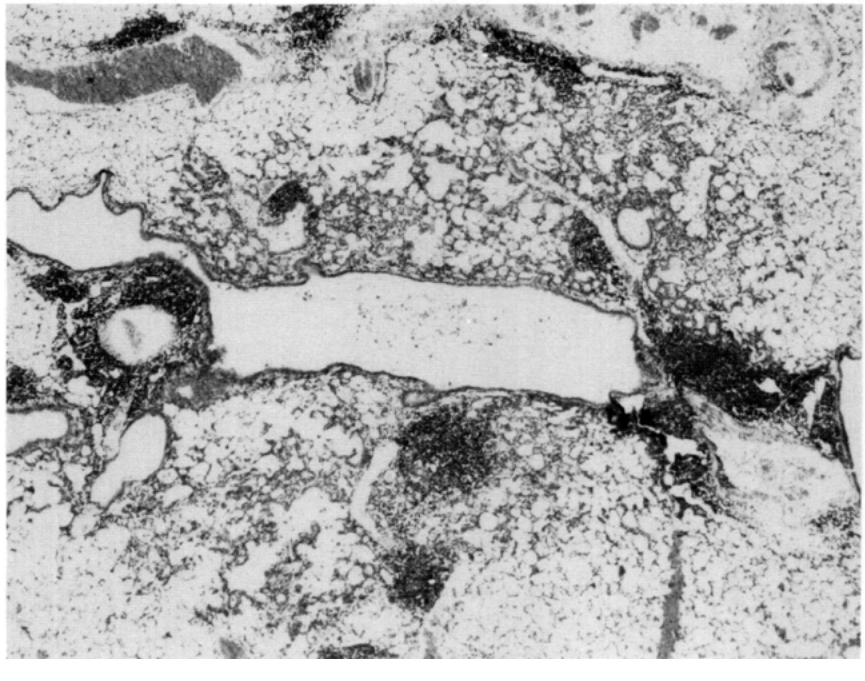

FIGURE 16. Peribronchial epithelial cell hypertrophy and hyperplasia; collections of macrophages in alveoli and perivascular and peribronchial lymphoid hyperplasia in the lung (H & E, ×52).

obliterated by a single or multiloculated cyst (Fig. 11). Cysts often contained clear fluid or blood. The ovarian stroma surrounding the cyst was frequently fibrotic and heavily pigmented with the products of blood breakdown.

Uterus. Distention of a segment or both uterine horns was a common gross observation. Endometrial glands in such cases were hyperplastic and cystic (Fig. 12). Varying degrees of stromal hyperplasia accompanied the cystic hyperplasia.

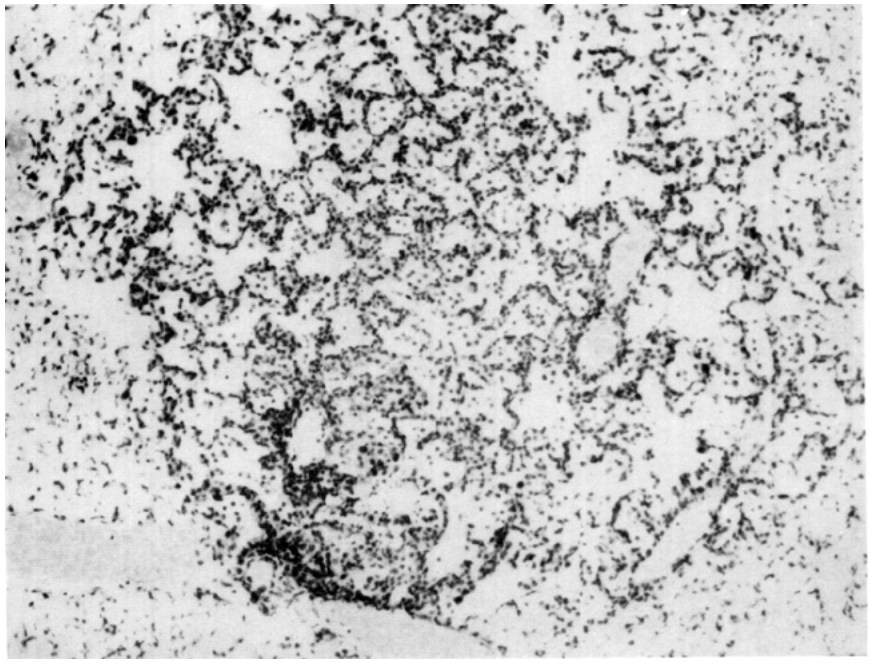

FIGURE 17. Hypertrophy of alveolar epithelial cells that rest on pre-existing alveolar walls. Compression of adjacent pulmonary tissue is not significant (H & E, ×260).

Integumentary System

Clitoral Gland. Enlargement of the clitoral gland, a common gross finding in treated and nontreated mice, was caused by dilatation, inflammation, or abscessation of the gland (Fig. 13). Neoplasms were not observed in our studies.

Mammary Glands. Inflammation and duct ectasia were common near skin paint sites.

Skin. Inflammatory lesions not related to treatment were frequently observed. These lesions were usually mild and consisted of slight inflammatory cell infiltration of hair follicles or were associated with hair or vegetable foreign bodies in the dermis (Fig. 14). Epithelial hyperplasia, erosion, ulceration, and active chronic inflammation were common at or near skin paint sites. These lesions are difficult to diagnose, since regenerative attempts on the part of the host need to be differentiated from neoplastic changes. A more complete description of such lesions has been reported (*7*).

Hematopoietic System

Lymph Nodes. Lymphocytic and plasmocytic hyperplasias were the most common cause of enlarged lymph nodes. Granulomatous inflammation was observed in nodes near areas of chronic or active-chronic inflammation. The cortical architecture of involved lymph nodes was obliterated by hyperplastic lymphoid tissue traversed by prominent bands of histiocytes and juvenile connective tissue. Medullary sinusoids were dilated with histiocytes.

Spleen. Hematopoietic cell hyperplasia (granulocytic and erythrocytic) and lymphoid hyperplasia were common causes of splenic enlargement. Such reactions were common in tumor-bearing mice and in mice with inflammatory processes elsewhere in the body. When the granulocytic hyperplasias are florid, their differentiation from myelogenous leukemia may be necessary (*4*). Amyloidlike deposits were often associated with the lesions. They involved the peripheral portion of splenic follicules and extended into the red pulp (Fig. 15).

Other incidental findings included focal fibrosis of the spleen and accessory splenic tissue, found usually in the mesentery near the pancreas.

Respiratory System

Lung. Inflammatory reactions included perivascular and peribronchial lymphocytic, and plasmocytic infiltrates, and focal or diffuse areas of chronic, or active-chronic inflammation. At times, they appeared as small granulomas. Lesions in some cases had a propensity for terminal bronchioles and adjacent alveoli. Peribronchiolar alveolar lining cells were hypertrophied, and interstitial areas were thickened by connective tissue proliferation and inflammatory cell infiltration (Fig. 16). Also observed were small focal collections of histiocytes, usually located in alveoli near the pleura. These histological features were difficult to differentiate from those described for late-stage Sendai virus infections (*8,9*)

Focal alveolar cell hyperplasia, felt to be a precursor lesion to alveolar/bronchiolar neoplasms, was infrequently encountered (Fig. 17).

Summary

Ovarian cysts, cystic endometrial hyperplasia, and mild glomerulonephritis were the most frequently encountered lesions in this survey. An apparent low incidence level of a wide variety of other naturally occurring lesions were found to involve several organ systems.

The material has been funded wholly or in part by the United States Environmental Protection Agency under contract 68-03-3170 to Pathology Associates, Inc. It has been subject to the Agency's review and it has been approved for publication as an EPA document. Mention of trade names or commercial products does not constitute endorsement or recommendation for use.

REFERENCES

1. Boutwell, R. K. Some biological aspects of skin carcinogenesis. Progr. Exp. Tumor Res. 4: 207–250 (1964).
2. DiGiovanni, J., Slaga, T. J., and Boutwell, R. K. Comparison of the tumor initiating activity of 7,12-dimethylbenz(a)anthracene and benzo(a)pyrene in female SENCAR and CD-1 mice. Carcinogenesis 1: 381–389 (1980).
3. Dunn, T. B. Amyloidosis in mice. In: Pathology of Laboratory Rats and Mice (E. Cotchin and F. J. C. Roe, Eds.), Blackwell Scientific Publications, Oxford, 1967, pp. 149–179.
4. Long, R. R., Knutsen, G. L., and Robinson, M. Myeloid hyperplasia in the SENCAR mouse: differentiation from granulocytic leukemia. Environ. Health Perspect. 68: 117–123 (1986).
5. Dunn, T. B. Normal and pathologic anatomy of the adrenal gland of the mouse, including neoplasms. J. Natl. Cancer Inst. 44: 1323–1389 (1970).
6. Burek, J. D., Molello, J. A., and Warner, S. D. Selected nonneoplastic diseases. In: The Mouse in Biomedical Research, Vol. 2 (H. Foster, J. Small, and J. Fox, Eds.), Academic Press, New York, 1982, pp. 425–440.
7. Knutsen, G. L., Kovatch, R. M., and Robinson, M. Gross and microscopic changes in the SENCAR lung and skin. Environ. Health Perspect. 68: 91–104 (1986).
8. Appell, L. H., Kovatch, R. M., Reddecliff, J. M., and Gerone, P. J. Pathogenesis of Sendai virus infection in mice. Am. J. Vet. Res. 32: 1835–1841 (1971).
9. Ward, J. M. Naturally occurring Sendai virus disease of mice. Lab. Anim. Sci. 24: 938–942 (1974).